IEEE Open Journal of Signal Processing

Received 13 October 2025; revised 18 November 2025; accepted 10 December 2025. Date of publication 15 December 2025; date of current version 16 January 2026. The review of this article was arranged by Associate Editor Fangqing Wen.

Digital Object Identifier 10.1109/OJSP.2025.3644786

Direction of Arrival Estimation for the Coexistence of Uncorrelated and Coherent Signals via Rotation Spatial Differencing Method

PENG LUO [1,2,3], BOYU PANG [1,2,3], DEFENG WU [4,5,6] (Senior Member, IEEE), AND W. ZENG [1,2,3]

[1]Institute of Marine Equipment, Shanghai Jiao Tong University, Shanghai 200240, China
[2]Shanghai Chang Xing Ocean Laboratory, Shanghai 201913, China
[3]School of Naval Architecture, Ocean, and Civil Engineering, Shanghai Jiao Tong University, Shanghai 200240, China
[4]School of Marine Engineering, Jimei University, Xiamen 361021, China
[5]Fujian Institute of Innovation for Marine Equipment Detection and Remanufacturing Industrial Technology, Xiamen 361021, China
[6]Fujian Provincial Key Laboratory of Naval Architecture and Ocean Engineering, Xiamen 361021, China

CORRESPONDING AUTHOR: W. ZENG (email: roberttseng@126.com).

This work was supported in part by the Oceanic Interdisciplinary Program of Shanghai Jiao Tong University under Grant SL2023ZD106 and in part by Shanghai City Research Foundation under Grant 24GFC-GB02-2004 and Grant GO3230007.

ABSTRACT This paper presents a novel direction of arrival (DOA) estimation method via rotation spatial differencing technique that offers high resolution, robustness, and stable performance. To suppress external environmental noise and improve estimation accuracy, a new modified covariance matrix is constructed using a rotation matrix technique. Additionally, a spatial differencing matrix is built with neighboring subarrays to achieve signal decoherence. Due to the introduction of the new modified covariance matrix, the differencing matrix has a new feature without compromising the array flow pattern, leading to improved spatial differencing. Finally, a multiple signal classification (MUSIC) spectral search algorithm using the singular value decomposition (SVD) is applied to accurately localize both uncorrelated and coherent signals at once, which greatly facilitates the DOA estimation process. Experimental results demonstrate that the proposed method delivers superior DOA estimation performance, providing accurate and stable signal direction estimation.

INDEX TERMS Array signal processing, coherent signals, direction of arrival (DOA), sensor array.

I. INTRODUCTION

With the rapid development of the Information Age, wireless mobile communication services are expanding at an explosive pace, driving new demands for communication technology [1]. Adaptive antenna array technology, with its ability to significantly enhance system performance, increase capacity, and extend coverage, has become the focus of current research [2], [3], [4], [5]. This technology involves arranging sensors in specific spatial configurations to form an array. These sensor arrays are then used to detect spatial signals and estimate key parameters, such as the number of signals, their propagation direction, and location. Direction of arrival (DOA) estimation is a critical research area within array signal processing, with wide-ranging applications in fields such as radio, communication, radar, sonar, navigation and more [6], [7], [8], [9], [10], [11], [12].

DOA estimation refers to the determination of the incidence angle of the signals, i.e., the location of the signal sources, through signal processing techniques. This technique utilizes the received signals from the antenna array to analyze the phase and amplitude information of the signals and process them to ultimately determine the DOA of signals. Commonly used DOA estimation methods include subspace-based [13], [14], sparse-based [15], [16] and maximum likelihood methods [17], [18]. Among them, the multiple signal classification (MUSIC) algorithm has received considerable attention from researchers due to its super-resolution and robustness [19], [20], [21]. However, the complexity of the electromagnetic

environment and the multipath propagation of signals, which leads to high signal coherence, greatly reducing the performance of the MUSIC algorithm [22].

In the radio signal transmission process, the multipath effect is common. This occurs when the signal encounters terrain, obstacles, and other features, leading to reflection, diffraction, and scattering, which results in multiple propagation paths for the signal. The components of the signal arrive at the receiver at different times, and their respective phases combine, causing interference, so that the original signal distortion, or to produce errors. In addition, the independence of the signals can be damaged by the multipath effect and cochannel interference, resulting in signal coherence. When the signal is coherent, the rank of the covariance matrix of the data received by the array will be deficient, which obviously results in the dimension of the signal subspace being smaller than the number of signal sources, thus spreading the signal subspace into the noise subspace. At this time, the orientation vector of the coherent source is not completely orthogonal to the noise subspace, making it impossible to accurately estimate the direction of the signal source [23]. Therefore, the traditional DOA estimation method is difficult to deal with such signals effectively [24]. To solve such problems, methods such as spatial smoothing [25] and Toeplitz matrix reconstruction [26] have been proposed to realize the decoherence and decorrelation of coherent signals. However, conventional spatial smoothing algorithms result in significant array aperture loss, which greatly reduces the number of signals they can estimate. While the traditional Toeplitz matrix reconstruction method does not cause aperture loss, its susceptibility to noise interference and poor estimation accuracy make it unsuitable for contemporary applications that require precise localization.

Therefore, building on this foundation, researchers have successively proposed many high-performance DOA estimation methods. A cumulants-based Toeplitz matrices reconstruction method is proposed in [27], where the cumulant elements are arranged to construct the Toeplitz matrix for estimating the DOA. To achieve accurate tracking coherent acoustic targets, a DOA tracking algorithm based on acoustic vector sensor pseudo-smoothing is designed in [28]. This algorithm utilizes higher-order cumulants instead of the traditional second-order covariance matrix to reduce the effect of Gaussian noise, and is also used for pseudo-smoothing methods to achieve the decoherence of the coherent signal. While these methods are effective in reducing the interference of noise on the DOA estimation and accurately estimates the angle of incidence of the coherent signal, they significantly increase the computational complexity of the algorithm due to the use of the higher-order cumulants. Furthermore, with the rapid development of artificial intelligence, deep learning is also increasingly being applied to DOA estimation [29]. In [30], a data-driven DOA estimation method is proposed. It utilizes the deep augmented MUSIC algorithm to address the problem of the sensitivity to model mismatch, and accurately estimate the locations of coherent signals. However, this requires a lot of data and time for training, and has high requirements for computer computational power. In addition, these methods only consider coherent or correlated signals and do not take into account the mixing of coherent and uncorrelated signals.

To address the coexistence of both uncorrelated and coherent signals, an effective spatial differencing method is proposed in [31], which first estimates the uncorrelated signals by traditional subspace-based method. Then, the estimation of the coherent signal is realized using spatial differencing methods. In order to improve the decoherence ability of the algorithm, an improved spatial differencing method is proposed in [23], which utilizes the neighboring subarrays to construct the spatial differencing matrix and improves the estimation performance. On this foundation, it is further improved in [32] by constructing the forward-backward spatial differencing matrix, further enhancing the estimation accuracy. All of these methods are able to accurately and efficiently estimate the incident directions of mixed signals, but they need to perform two spectral searches, one for uncorrelated signals and one for coherent signals, which increases the computational load and makes the process cumbersome.

Therefore, based on previous work, this paper further analyzes and explores an efficient, fast, high-resolution, accurate, and stable DOA estimation method. The main contributions of this paper are as follows:

1) We propose a modified covariance matrix construction method and integrate it into the spatial differencing technique, endowing the approach with the following advantages: i) The estimation accuracy and stability are significantly improved. ii) The method can estimate more coherent signals using fewer subarrays compared to existing techniques. iii) The search process is simplified, enabling joint DOA estimation of both coherent and uncorrelated signals via a one-time spectral search.
2) Through rigorous theoretical analysis and comprehensive comparative simulations, we demonstrate the superior performance of our method over existing techniques in terms of estimation precision, computational efficiency, and practical applicability. Furthermore, we conduct extensive experimental validations and multi-round comparative studies to thoroughly investigate the performance characteristics and influencing factors of our DOA estimation approach, with results consistently confirming its advantages over state-of-the-art methods.

The remainder of the paper is organized as follows: Section II introduces the symbols and correlation coefficients involved and constructs the signal model required for the study. Section III presents the DOA estimation method proposed in this paper and provides a theoretical justification for it. Section IV analyzes and validates the superiority of the proposed method through two experiments, examining the factors that affect its performance. Section V summarizes the paper, discusses the shortcomings of the existing work, and outlines directions for future research.

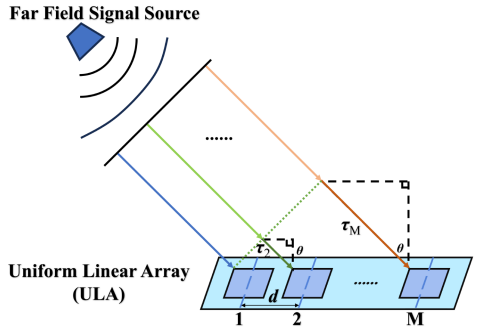

FIGURE 1. ULA model.

II. PROBLEM FORMULATION

A. SYMBOL DESCRIPTION

For ease of reading and understanding, the meanings of the symbols used in this paper are explained as follows: The symbol j represents the imaginary unit, i.e., $\sqrt{-1} = j$; $(\cdot)^{\mathrm{H}}$, $(\cdot)^{\top}$ and $(\cdot)^{*}$ denote the conjugate transpose, transpose and conjugate, respectively; $E[\cdot]$ denotes the mathematical expectation; $|\cdot|$ denotes the absolute value. Additionally, bold uppercase letters are used to represent matrices, and bold lowercase letters are used to represent vectors.

B. CORRELATION COEFFICIENT

The correlation coefficient is generally used to indicate the degree of correlation between signals and can be expressed as follows:

$$\zeta_{ij} = \frac{E\left[\left(s_i(t) - E\left[s_i(t)\right]\right)\left(s_j(t) - E\left[s_j(t)\right]\right)^{*}\right]}{\sqrt{E\left[|s_i(t) - E\left[s_i(t)\right]|^2\right]E\left[|s_j(t) - E\left[s_j(t)\right]|^2\right]}} \quad (1)$$

where ζ_{ij} is the correlation coefficient between $s_i(t)$ and $s_j(t)$ with $|\zeta_{ij}| \leq 1$. When $|\zeta_{ij}| = 0$, $s_i(t)$ and $s_j(t)$ are uncorrelated; $0 < |\zeta_{ij}| < 1$, $s_i(t)$ and $s_j(t)$ are correlated; and when $|\zeta_{ij}| = 1$, $s_i(t)$ and $s_j(t)$ are coherent.

C. SIGNAL MODEL

Consider a uniform linear array (ULA) consisting of M isotropic array sensors receiving K uncorrelated and coherent far-field narrowband mixed signals $\mathbf{s}(t) = [s_1(t), s_2(t), \ldots, s_L(t), s_{L+1}(t), \ldots, s_{L+Q-1}(t), s_K(t)]^{\top} \in \mathbb{C}^{K\times 1}$ with signal wavelength λ, where the front L signals are coherent and the remaining $Q = K - L$ signals are uncorrelated as in Fig. 1. The incidence angle of signals is $\theta_k, (k = 1, 2, \ldots, K)$ and the powers are all σ_s^2. Meanwhile, array antennas and far-field sources are in the same plane. The output signal of the mth array sensor can be expressed as:

$$x_m(t) = \sum_{k=1}^{K} g_{mk} s_k(t - \tau_{m,k}) + n_m(t), m = 1, 2, \ldots, M \quad (2)$$

where g_{mk} denotes the gain of the kth signal at the mth array sensor; s_k is the kth signal source; $n_m(t)$ is the additive noise received at the mth array sensor; and $\tau_{m,k}$ is the delay from the kth source to the mth array sensor with respect to the reference array sensor. Since the individual array sensors in the array are isotropic and have the same gain, therefore $g_{mk} = 1$. And the sources are far-field narrow-band signals, it can be approximated as a plane wave incident to the ULA; meanwhile, since the propagation time through the ULA aperture is much shorter than the inverse of the signal bandwidth, the difference of the signal envelope in at each array sensor is negligible. Therefore, assuming that the interval between the array sensors is and using the first array sensor as the reference array sensor, it can be obtained that:

$$s_k(t - \tau_{m,k}) \approx s_k(t) e^{-j\frac{2\pi}{\lambda}(m-1)d\sin(\theta_k)} \quad (3)$$

Therefore, (2) can be transformed to:

$$x_m(t) = \sum_{k=1}^{L} s_k(t) e^{-j\frac{2\pi}{\lambda}(m-1)d\sin(\theta_k)} + \sum_{k=L+1}^{L+Q} s_k(t) e^{-j\frac{2\pi}{\lambda}(m-1)d\sin(\theta_k)} + n_m(t) \quad (4)$$

Then, the output of the array at time t, $\mathbf{x}(t) = [x_1(t), x_2(t), \ldots, x_M(t)]^{\top} \in \mathbb{C}^{M\times 1}$, is given by:

$$\begin{aligned}\mathbf{x}(t) &= \sum_{k=1}^{L} s_k(t)\mathbf{a}(\theta_k) + \sum_{k=L+1}^{L+Q} s_k(t)\mathbf{a}(\theta_k) + \mathbf{n}(t) \\ &= s_1(t)\sum_{k=1}^{L}\alpha_k\mathbf{a}(\theta_k) + \sum_{k=L+1}^{L+Q} s_k(t)\mathbf{a}(\theta_k) + \mathbf{n}(t) \\ &= \mathbf{A}_c\mathbf{s}_c(t) + \mathbf{A}_u\mathbf{s}_u(t) + \mathbf{n}(t)\end{aligned} \quad (5)$$

where $\mathbf{a}(\theta_k) = [1, e^{-j\frac{2\pi}{\lambda}d\sin(\theta_k)}, \ldots, e^{-j\frac{2\pi}{\lambda}(M-1)d\sin(\theta_k)}]^{\top} \in \mathbb{C}^{M\times 1}$ is the steering vector; $\mathbf{n}(t) = [n_1(t), n_2(t), \ldots, n_M(t)]^{\top} \in \mathbb{C}^{M\times 1}$ is the Gaussian white noise received by the ULA from the external environment with power σ_n^2. α_k denotes the composite fading factor, which generally has $|\alpha_k| \leq 1$, and $\alpha_1 = 1$. $\mathbf{A}_c = [\mathbf{a}(\theta_1), \mathbf{a}(\theta_2), \ldots, \mathbf{a}(\theta_L)] \in \mathbb{C}^{M\times L}$, $\mathbf{A}_u = [\mathbf{a}(\theta_{L+1}), \mathbf{a}(\theta_{L+2}), \ldots, \mathbf{a}(\theta_{L+Q})] \in \mathbb{C}^{M\times Q}$ and $\mathbf{A} = [\mathbf{A}_c, \mathbf{A}_u] \in \mathbb{C}^{M\times K}$ are the array manifold matrix of the coherent signals, uncorrelated signals and all signals, respectively. $\mathbf{s}_c(t) = [s_1(t), s_2(t), \ldots, s_L(t)]^{\top} = [\alpha_1, \alpha_2, \ldots, \alpha_L]^{\top} s_1(t) \in \mathbb{C}^{L\times 1}$, $\mathbf{s}_u(t) = [s_{L+1}(t), s_{L+2}(t), \ldots, s_{L+Q}(t)]^{\top} \in \mathbb{C}^{Q\times 1}$, $\mathbf{s}(t) = [\mathbf{s}_c(t); \mathbf{s}_u(t)] \in \mathbb{C}^{K\times 1}$ are the coherent signal matrix, the uncorrelated signal matrix, and the total signal matrix, respectively. In addition, the general form of the composite fading factor is $\alpha_k = \rho_k e^{j\delta\varphi_k}$, where ρ_k and φ_k are the amplitude change and phase change, respectively.

III. DOA ESTIMATION

This section will detail the design flow of the proposed method, which will begin with reconstructing a modified covariance matrix on the traditional covariance matrix of the array data using the rotation matrix method to initially decoherence the signal and increase the signal resolution. Subsequently, the modified covariance matrix of the array

data is further processed to construct a differencing matrix that contains all signals without rank loss using a spatial differencing method. Finally, the directions of all the signal sources are estimated using the singular value decomposition (SVD)-based MUSIC spectral search algorithm.

In the first step, the covariance matrix of the array data is estimated using the maximum likelihood method:

$$\mathbf{R}_x = E\left[\mathbf{x}(t)\mathbf{x}^{\mathrm{H}}(t)\right] \approx \mathbf{X}\mathbf{X}^{\mathrm{H}}/N \tag{6}$$

where N is the number of snapshots, and $\mathbf{X} = [\mathbf{x}(1), \mathbf{x}(2), \ldots, \mathbf{x}(N)] \in \mathbb{C}^{M\times N}$ is the output data matrix containing N snapshots collected by the ULA. Subsequently, it is further processed to obtain $\bar{\mathbf{R}}_x$:

$$\bar{\mathbf{R}}_x = \mathbf{R}_x + \mathbf{J}\mathbf{R}_x^* \tag{7}$$

where $\mathbf{J} \in \mathbb{R}^{M\times M}$ is the exchange matrix (also known as the backward identity matrix), wherein the anti-diagonal elements are all ones and all other elements are exclusively zero.

Furthermore, $\mathbf{J}\mathbf{R}_x^*$ is equivalent to a 90° counterclockwise rotation of $\mathbf{R}_x$, i.e., $\mathbf{J}\mathbf{R}_x^* = \mathrm{rot90}(\mathbf{R}_x)$.

Remark 1: The modified covariance matrix $\bar{\mathbf{R}}_x$ from (7) provides preliminary decoupling of coherent signals with performance comparable to conventional forward/backward averaging. Combined with the spatial differencing method, it further enhances decorrelation and enables simultaneous DOA estimation for mixed signals.

Next, the modified covariance matrix $\bar{\mathbf{R}}_x$ is split into P overlapping sub-matrices, where the pth sub-matrix is:

$$\mathbf{R}_p = \mathbf{K}_p\bar{\mathbf{R}}_x\mathbf{K}_p^{\mathrm{H}}, \quad p = 1, 2, \ldots, P \tag{8}$$

where $\mathbf{K}_p = [\mathbf{0}_{(M-P+1)\times(p-1)}, \mathbf{I}_{(M-P+1)}, \mathbf{0}_{(M-P+1)\times(P-p)}] \in \mathbb{R}^{(M-P+1)\times M}$ is the selection matrix; $\mathbf{I}_{(M-P+1)}$ is an $(M-P+1)$-dimensional unit matrix.

Remark 2: To guarantee that the ULA can accurately estimate the DOA of coherent signals, as in the classical smoothing method, the number of array sensors in each subarray must be more than the number of coherent signals.

Then, based on the obtained new modified covariance matrix, construct a spatial differencing matrix:

$$\begin{aligned}\mathbf{H} &= \frac{1}{P}\sum_{p=1}^{P}(\mathbf{R}_{p-1} - \mathbf{J}_{M-P+1}\mathbf{R}_p^*\mathbf{J}_{M-P+1}) \\ &= \frac{1}{P}\sum_{p=1}^{P}(\mathbf{K}_{p-1}\bar{\mathbf{R}}_x\mathbf{K}_{p-1}^{\mathrm{H}} \\ &\quad - \mathbf{J}_{M-P+1}(\mathbf{K}_p\bar{\mathbf{R}}_x\mathbf{K}_p^{\mathrm{H}})^*\mathbf{J}_{M-P+1})\end{aligned} \tag{9}$$

where $\mathbf{J}_{M-P+1}$ denotes the anti-diagonal matrix of dimension $M-P+1$. Furthermore, for the specific case of $p = 1$, $\mathbf{R}_1$ replaces the undefined $\mathbf{R}_0$ in the spatial differencing operation, with the corresponding selection matrix defined as $\mathbf{K}_0 = \mathbf{K}_1 = [\mathbf{I}_{(M-P+1)}, \mathbf{0}_{(M-P+1)\times(P-1)}]$.

Remark 3: Note that the algorithm is fundamentally based on spatial differencing between adjacent subarrays. For the first differencing term, this originally yields the expression $\mathbf{R}_0 - \mathbf{J}_{M-P+1}\mathbf{R}_1\mathbf{J}_{M-P+1}$. To ensure numerical stability, we substitute $\mathbf{R}_0$ with $\mathbf{R}_1$, resulting in the modified operation $\mathbf{R}_1 - \mathbf{J}_{M-P+1}\mathbf{R}_1\mathbf{J}_{M-P+1}$. This spatial differencing approach not only effectively achieves decorrelation of coherent sources but also inherently suppresses noise through its subtractive nature, thereby significantly enhancing the robustness and stability of the algorithm.

Finally, the constructed new spatial differencing matrix $\mathbf{H}$ is brought into the conventional MUSIC spectral search algorithm to estimate all the DOA of the coherent and uncorrelated signals accurately.

Theorem 1: Assume that there are a total of K narrowband far-field signals incident into the ULA of element M. Without loss of generality, the first L signals are assumed to be coherent, while the remaining Q signals are uncorrelated; the angles of incidence are denoted by θ_k, $(k = 1, 2, \ldots, K)$, and the power is all σ_s^2. The newly constructed spatial differencing matrix $\mathbf{H}$ in (9) exhibits no rank loss, with its rank equal to the total number of signals.

Proof: From (7), $\bar{\mathbf{R}}_x$ consists of the original data covariance matrix $\mathbf{R}_x$ and the rotation covariance matrix $\mathbf{J}\mathbf{R}_x^*$. Thus $\mathbf{H}$ can be divided into two parts, one with respect to $\mathbf{R}_x$ and the other with respect to $\mathbf{J}\mathbf{R}_x^*$, denoted $\mathbf{H}_1$, $\mathbf{H}_2$, respectively, i.e.:

$$\begin{aligned}\mathbf{H} &= \frac{1}{P}\sum_{p=1}^{P}(\mathbf{K}_{p-1}\mathbf{R}_x\mathbf{K}_{p-1}^{\mathrm{H}} \\ &\quad - \mathbf{J}_{M-P+1}(\mathbf{K}_p\mathbf{R}_x\mathbf{K}_p^{\mathrm{H}})^*\mathbf{J}_{M-P+1}) \\ &\quad + \frac{1}{P}\sum_{p=1}^{P}(\mathbf{K}_{p-1}\mathbf{J}\mathbf{R}_x^*\mathbf{K}_{p-1}^{\mathrm{H}} \\ &\quad - \mathbf{J}_{M-P+1}(\mathbf{K}_p\mathbf{J}\mathbf{R}_x^*\mathbf{K}_p^{\mathrm{H}})^*\mathbf{J}_{M-P+1}) \\ &= \mathbf{H}_1 + \mathbf{H}_2\end{aligned} \tag{10}$$

where $\mathbf{H}_1 = \frac{1}{P}\sum_{p=1}^{P}(\mathbf{K}_{p-1}\mathbf{R}_x\mathbf{K}_{p-1}^{\mathrm{H}} - \mathbf{J}_{M-P+1}(\mathbf{K}_p\mathbf{R}_x\mathbf{K}_p^{\mathrm{H}})^*\mathbf{J}_{M-P+1})$ and $\mathbf{H}_2 = \frac{1}{P}\sum_{p=1}^{P}(\mathbf{K}_{p-1}\mathbf{J}\mathbf{R}_x^*\mathbf{K}_{p-1}^{\mathrm{H}} - \mathbf{J}_{M-P+1}(\mathbf{K}_p\mathbf{J}\mathbf{R}_x^*\mathbf{K}_p^{\mathrm{H}})^*\mathbf{J}_{M-P+1})$. Furthermore, $\mathbf{H}_1$ is fully argued and analyzed in Ref. [23], [31]. And the following section will analyze the remaining part $\mathbf{H}_2$ according to those literature.

Based on the previous analysis, $\mathbf{J}\mathbf{R}_x^*$ can be decomposed into:

$$\begin{aligned}\mathbf{J}\mathbf{R}_x^* &= \mathbf{J}\left(\mathbf{R}_N + \mathbf{R}_{NT} + \sigma_n^2\mathbf{I}_M\right)^* \\ &= \mathbf{J}\left(\mathbf{A}_u\mathbf{R}_u\mathbf{A}_u^{\mathrm{H}} + \mathbf{A}_c\mathbf{R}_c\mathbf{A}_c^{\mathrm{H}} + \sigma_n^2\mathbf{I}_M\right)^*\end{aligned} \tag{11}$$

where $\mathbf{R}_N = \mathbf{A}_u\mathbf{R}_u\mathbf{A}u^{\mathrm{H}}$ and $\mathbf{R}_{NT} = \mathbf{A}_c\mathbf{R}_c\mathbf{A}_c^{\mathrm{H}}$, with $\mathbf{R}_u = E[\mathbf{s}_u(t)\mathbf{s}_u^{\mathrm{H}}(t)]$ and $\mathbf{R}_c = E[\mathbf{s}_c(t)\mathbf{s}_c^{\mathrm{H}}(t)]$ being the covariance matrices of the uncorrelated and coherent signals, respectively.

According to (10) and (11), $\mathbf{H}_2$ can be divided into two parts, uncorrelated and coherent signals, as follows:

$$\mathbf{H}_2 = \frac{1}{P}\sum_{p=1}^{P}\left(\left(\mathbf{J}\mathbf{R}_x^*\right)_{p-1} - \mathbf{J}_{M-P+1}\left(\mathbf{J}\mathbf{R}_x^*\right)_p^*\mathbf{J}_{M-P+1}\right)$$

$$= \frac{1}{P}\sum_{p=1}^{P}\left(\left(\mathbf{J}\mathbf{R}_N^*\right)_{p-1} - \mathbf{J}_{M-P+1}\left(\mathbf{J}\mathbf{R}_N^*\right)_p^*\mathbf{J}_{M-P+1}\right)$$
$$+ \frac{1}{P}\sum_{p=1}^{P}\left(\left(\mathbf{J}\mathbf{R}_{NT}^*\right)_{p-1} - \mathbf{J}_{M-P+1}\left(\mathbf{J}\mathbf{R}_{NT}^*\right)_p^*\mathbf{J}_{M-P+1}\right)$$
$$= \frac{1}{P}\sum_{p=1}^{P}\left(\mathbf{W}_p + \mathbf{F}_p\right) \tag{12}$$

where $\mathbf{W}_p = (\mathbf{J}\mathbf{R}_N^*)_{p-1} - \mathbf{J}_{M-P+1}(\mathbf{J}\mathbf{R}_N^*)_p^*\mathbf{J}_{M-P+1}$ is the uncorrelated signal part; $\mathbf{F}_p = (\mathbf{J}\mathbf{R}_{NT}^*)_{p-1} - \mathbf{J}_{M-P+1}(\mathbf{J}\mathbf{R}_{NT}^*)_p^*\mathbf{J}_{M-P+1}$ is the coherent signal part.

Firstly, analyzing the uncorrelated part $\mathbf{W}_p$, according to (9) and (10), $(\mathbf{J}\mathbf{R}_N^*)_{p-1}$ can be converted to:

$$\begin{aligned}\left(\mathbf{J}\mathbf{R}_N^*\right)_{p-1} &= \mathbf{K}_{p-1}\mathbf{J}\mathbf{R}_N^*\mathbf{K}_{p-1}^{\mathrm{H}}\\ &= \mathbf{K}_{p-1}\mathbf{J}\left(\mathbf{A}_u\mathbf{R}_u\mathbf{A}_u^{\mathrm{H}}\right)^*\mathbf{K}_{p-1}^{\mathrm{H}}\\ &= \mathbf{K}_{p-1}\mathbf{J}\mathbf{A}_u^*\mathbf{R}_u^*\left(\mathbf{A}_u^*\right)^{\mathrm{H}}\mathbf{K}_{p-1}^{\mathrm{H}}\end{aligned} \tag{13}$$

Due to $\mathbf{J}\mathbf{A}_u^* = \mathbf{A}_u\mathbf{\Theta}^{M-1}$ with $\mathbf{\Theta} = \mathrm{diag}\{e^{j\frac{2\pi}{\lambda}d\sin(\theta_{L+1})}, \ldots, e^{j\frac{2\pi}{\lambda}d\sin(\theta_{L+Q})}\}$, (13) can then be further simplified to:

$$\begin{aligned}\left(\mathbf{J}\mathbf{R}_N^*\right)_{p-1} &= \mathbf{K}_{p-1}\mathbf{A}_u\mathbf{\Theta}^{M-1}\mathbf{R}_u^*\left(\mathbf{A}_u^*\right)^{\mathrm{H}}\mathbf{K}_{p-1}^{\mathrm{H}}\\ &= \mathbf{A}_{u1}\mathbf{\Theta}^{M-1}\mathbf{R}_u^*\left(\mathbf{A}_{u1}^*\right)^{\mathrm{H}}\end{aligned} \tag{14}$$

where $\mathbf{A}_{u1} = \mathbf{K}_{p-1}\mathbf{A}_u$.

Next, the remaining portion of the uncorrelated signal $\mathbf{J}_{M-P+1}(\mathbf{J}\mathbf{R}_N^*)_p^*\mathbf{J}_{M-P+1}$ will be analyzed:

Similarly, expand it according to (10) as:

$$\begin{aligned}&\mathbf{J}_{M-P+1}(\mathbf{J}\mathbf{R}_N^*)_p^*\mathbf{J}_{M-P+1}\\ &= \mathbf{J}_{M-P+1}\left(\mathbf{K}_p\mathbf{J}\left(\mathbf{A}_u\mathbf{R}_u\mathbf{A}_u^{\mathrm{H}}\right)\mathbf{K}_p^{\mathrm{H}}\right)\mathbf{J}_{M-P+1}\end{aligned} \tag{15}$$

From $\mathbf{J}\mathbf{A}_u^* = \mathbf{A}_u\mathbf{\Theta}^{M-1}$, it follows that $(\mathbf{J}\mathbf{A}_u^*)^* = (\mathbf{A}_u\mathbf{\Theta}^{M-1})^* = \mathbf{A}_u^*\mathbf{\Theta}^{1-M}$. Furthermore, $\mathbf{K}_p\mathbf{A}_u = \mathbf{A}_{u1}\mathbf{\Theta}^*$. Therefore, (15) can be further simplified as:

$$\begin{aligned}&\mathbf{J}_{M-P+1}(\mathbf{J}\mathbf{R}_N^*)_p^*\mathbf{J}_{M-P+1}\\ &= \mathbf{J}_{M-P+1}\left(\mathbf{K}_p\left(\mathbf{A}_u^*\mathbf{\Theta}^{1-M}\mathbf{R}_u\mathbf{A}_u^{\mathrm{H}}\right)\mathbf{K}_p^{\mathrm{H}}\right)\mathbf{J}_{M-P+1}\\ &= \mathbf{J}_{M-P+1}\left(\mathbf{A}_{u1}^*\mathbf{\Theta}\mathbf{\Theta}^{1-M}\mathbf{R}_u\mathbf{\Theta}\mathbf{A}_{u1}^{\mathrm{H}}\right)\mathbf{J}_{M-P+1}\\ &= \mathbf{J}_{M-P+1}\left(\mathbf{A}_{u1}^*\mathbf{\Theta}^{3-M}\mathbf{R}_u\mathbf{A}_{u1}^{\mathrm{H}}\right)\mathbf{J}_{M-P+1}\end{aligned} \tag{16}$$

Once again, based on $\mathbf{J}_{M-P+1}\mathbf{A}_{u1}^* = \mathbf{A}_{u1}\mathbf{\Theta}^{M-P+2(p-2)}$, (16) further simplifies to:

$$\begin{aligned}&\mathbf{J}_{M-P+1}(\mathbf{J}\mathbf{R}_N^*)_p^*\mathbf{J}_{M-P+1}\\ &= \left(\mathbf{J}_{M-P+1}\mathbf{A}_{u1}^*\right)\mathbf{\Theta}^{3-M}\mathbf{R}_u\left(\left(\mathbf{A}_{u1}^{\mathrm{H}}\right)^*\mathbf{J}_{M-P+1}\right)^*\\ &= \mathbf{A}_{u1}\mathbf{\Theta}^{2(M-P+2(p-2))}\mathbf{\Theta}^{3-M}\mathbf{R}_u\left(\mathbf{A}_{u1}^*\right)^{\mathrm{H}}\\ &= \mathbf{A}_{u1}\mathbf{\Theta}^{(M-2P+4p-5)}\mathbf{R}_u\left(\mathbf{A}_{u1}^*\right)^{\mathrm{H}}\end{aligned} \tag{17}$$

Combining (14) and (17) yields:

$$\mathbf{W}_p = \mathbf{A}_{u1}\mathbf{\Theta}^{M-1}\left(\mathbf{R}_u^* - \mathbf{\Theta}^{(-2P+4p-4)}\mathbf{R}_u\right)\left(\mathbf{A}_{u1}^*\right)^{\mathrm{H}} \tag{18}$$

Next, the coherent signal $\mathbf{F}_p$ will be analyzed. Similar to the above steps, $(\mathbf{J}\mathbf{R}_{NT}^*)_{p-1}$ is first analyzed. Based on (11) and (12), it can be obtained:

$$\begin{aligned}\left(\mathbf{J}\mathbf{R}_{NT}^*\right)_{p-1} &= \mathbf{K}_{p-1}\mathbf{J}\mathbf{R}_{NT}^*\mathbf{K}_{p-1}^{\mathrm{H}}\\ &= \mathbf{K}\mathbf{K}_{p-1}\mathbf{J}\left(\mathbf{A}_c\mathbf{R}_c\mathbf{A}_c^{\mathrm{H}}\right)^*\mathbf{K}_{p-1}^{\mathrm{H}}\\ &= \mathbf{K}_{p-1}\mathbf{J}\mathbf{A}_c^*\mathbf{R}_c^*\left(\mathbf{A}_c^*\right)^{\mathrm{H}}\mathbf{K}_{p-1}^{\mathrm{H}}\end{aligned} \tag{19}$$

Let $\mathbf{s}_c(t) = \mathbf{b}s_1(t)$, where $\mathbf{b} = [\alpha_1, \alpha_2, \ldots, \alpha_L]^\top \in \mathbb{C}^{L\times 1}$ is the coherence coefficient vector. Then:

$$\mathbf{R}_c = E\left[\mathbf{s}_c(t)\mathbf{s}_c^{\mathrm{H}}(t)\right] = E\left[s_1(t)s_1^{\mathrm{H}}(t)\right]\mathbf{b}\mathbf{b}^{\mathrm{H}} = \sigma_s^2\mathbf{b}\mathbf{b}^{\mathrm{H}} \tag{20}$$

Bringing (20) into (19) gives:

$$\left(\mathbf{J}\mathbf{R}_{NT}^*\right)_{p-1} = \sigma_s^2\mathbf{K}_{p-1}\mathbf{J}\mathbf{A}_c^*\left(\mathbf{b}\mathbf{b}^{\mathrm{H}}\right)^*\left(\mathbf{A}_c^*\right)^{\mathrm{H}}\mathbf{K}_{p-1}^{\mathrm{H}} \tag{21}$$

By the property of $\mathbf{J}\mathbf{A}_c^* = \mathbf{A}_c\mathbf{\Phi}^{M-1}$ with $\mathbf{\Phi} = \mathrm{diag}\{e^{j\frac{2\pi}{\lambda}d\sin(\theta_1)}, \ldots, e^{j\frac{2\pi}{\lambda}d\sin(\theta_L)}\}$, a further transformation of (21) yields:

$$\begin{aligned}\left(\mathbf{J}\mathbf{R}_{NT}^*\right)_{p-1} &= \sigma_s^2\mathbf{K}_{p-1}\mathbf{A}_c\mathbf{\Phi}^{M-1}\left(\mathbf{b}\mathbf{b}^{\mathrm{H}}\right)^*\mathbf{A}_c^{*\mathrm{H}}\mathbf{K}_{p-1}^{\mathrm{H}}\\ &= \sigma_s^2\mathbf{A}_{c1}\mathbf{\Phi}^{M-1}\left(\mathbf{b}\mathbf{b}^{\mathrm{H}}\right)^*\left(\mathbf{A}_{c1}^*\right)^{\mathrm{H}}\end{aligned} \tag{22}$$

where $\mathbf{A}_{c1} = \mathbf{K}_{p-1}\mathbf{A}_c$.

Similarly, expand on the remaining parts $\mathbf{J}_{M-P+1}(\mathbf{J}\mathbf{R}_{NT}^*)_p^*\mathbf{J}_{M-P+1}$:

$$\begin{aligned}&\mathbf{J}_{M-P+1}(\mathbf{J}\mathbf{R}_{NT}^*)_p^*\mathbf{J}_{M-P+1}\\ &= \mathbf{J}_{M-P+1}\left(\mathbf{K}_p\mathbf{J}\left(\mathbf{A}_c\mathbf{R}_c\mathbf{A}_c^{\mathrm{H}}\right)\mathbf{K}_p^{\mathrm{H}}\right)\mathbf{J}_{M-P+1}\\ &= \sigma_s^2\mathbf{J}_{M-P+1}\left(\mathbf{K}_p\mathbf{J}\mathbf{A}_c\mathbf{b}\mathbf{b}^{\mathrm{H}}\mathbf{A}_c^{\mathrm{H}}\mathbf{K}_p^{\mathrm{H}}\right)\mathbf{J}_{M-P+1}\end{aligned} \tag{23}$$

Bringing $(\mathbf{J}\mathbf{A}_c^*)^* = (\mathbf{A}_c\mathbf{\Phi}^{M-1})^*$ into (23) yields:

$$\begin{aligned}&\mathbf{J}_{M-P+1}(\mathbf{J}\mathbf{R}_{NT}^*)_p^*\mathbf{J}_{M-P+1}\\ &= \sigma_s^2\mathbf{J}_{M-P+1}\left(\mathbf{K}_p\mathbf{A}_c^*\mathbf{\Phi}^{1-M}\mathbf{b}\mathbf{b}^{\mathrm{H}}\mathbf{A}_c^{\mathrm{H}}\mathbf{K}_p^{\mathrm{H}}\right)\mathbf{J}_{M-P+1}\\ &= \sigma_s^2\mathbf{J}_{M-P+1}\left(\mathbf{A}_{c1}^*\mathbf{\Phi}\mathbf{\Phi}^{1-M}\mathbf{b}\mathbf{b}^{\mathrm{H}}\mathbf{\Phi}\mathbf{A}_{c1}^{\mathrm{H}}\right)\mathbf{J}_{M-P+1}\end{aligned} \tag{24}$$

Based on $\mathbf{J}_{M-P+1}\mathbf{A}_{c1}^* = \mathbf{A}_{c1}\mathbf{\Phi}^{M-P+2(p-2)}$, bringing it to (24) and simplifying yields:

$$\begin{aligned}&\mathbf{J}_{M-P+1}(\mathbf{J}\mathbf{R}_{NT}^*)_p^*\mathbf{J}_{M-P+1}\\ &= \sigma_s^2\mathbf{A}_{c1}\mathbf{\Phi}^{2(M-P+2(p-2))}\mathbf{\Phi}^{3-M}\mathbf{b}\mathbf{b}^{\mathrm{H}}\left(\mathbf{A}_{c1}^*\right)^{\mathrm{H}}\\ &= \sigma_s^2\mathbf{A}_{c1}\mathbf{\Phi}^{(M-2P+4p-5)}\mathbf{b}\mathbf{b}^{\mathrm{H}}\left(\mathbf{A}_{c1}^*\right)^{\mathrm{H}}\end{aligned} \tag{25}$$

Bringing (22) and (25) into the $\mathbf{F}_p$ expression yields:

$$\begin{aligned}\mathbf{F}_p = \sigma_s^2\mathbf{A}_{c1}\mathbf{\Phi}^{M-1}&\left(\left(\mathbf{b}\mathbf{b}^{\mathrm{H}}\right)^*\right.\\ &\left.- \mathbf{\Phi}^{(-2P+4p-4)}\mathbf{b}\mathbf{b}^{\mathrm{H}}\right)\left(\mathbf{A}_{c1}^*\right)^{\mathrm{H}}\end{aligned} \tag{26}$$

Thus far, all the decomposition forms of uncorrelated and coherent signals in $\mathbf{H}_2$ have been enumerated. Since $\mathbf{\Theta}$ and $\mathbf{\Phi}$ are both diagonal matrices in complex form, it can be readily concluded that both $\mathbf{W}_p$ ($\theta \neq 0^\circ$) and $\mathbf{F}_p$ are full rank matrices. And the number of their ranks is equal to the number of signals.

The concludes the proof.

Remark 4: According to (18), when the DOA of uncorrelated signals is $\theta = 0^\circ$, the corresponding $e^{j\frac{2\pi}{\lambda}d\sin\theta} = 1$, which leads to rank deficiency in the matrix $\mathbf{W}_p$, thereby preventing effective detection of targets at 0°. In practical applications, however, two factors mitigate this issue. First, due to finite signal sampling, the covariance matrix is generally not a purely real diagonal matrix. Second, multiple methods can be employed to determine whether a signal is incident from the 0° direction. For example: 1. The presence of a target signal can be assessed by receiving the signal from the 0° direction and analyzing its power level; 2. The array can be slightly adjusted—first estimating the number of signals and roughly determining their DOAs, and then fine-tuning the array orientation to verify whether a target exists at 0°.

Next, this paper will use the classic MUSIC algorithm to estimate the DOA of the signal sources.

Firstly, the eigenvalues and eigenvectors of the signal and noise are obtained. Compared to the eigenvalue decomposition, the SVD is numerically more stable, and here the SVD will be used to decompose the spatial differencing matrix:

$$\mathbf{H} = \mathbf{U}\mathbf{\Sigma}\mathbf{V}^{\mathrm{H}} = \mathbf{U}_s\mathbf{\Sigma}_s\mathbf{V}_s^{\mathrm{H}} + \mathbf{U}_n\mathbf{\Sigma}_n\mathbf{V}_n^{\mathrm{H}} \tag{27}$$

where $\mathbf{U}$ for left singular vector matrix is a column-orthogonal matrix containing the left singular vectors of $\mathbf{H}$. These vectors form the basis of the signal and noise subspaces and are commonly used to distinguish signal from noise; $\mathbf{U}_s$ is the signal subspace and $\mathbf{U}_n$ is the noise subspace. $\mathbf{\Sigma}$ is a singular value diagonal matrix that contains the singular values of $\mathbf{H}$. The singular values are arranged in order of magnitude, with the first K larger singular values $\mathbf{\Sigma}_s$ corresponding to the signal subspace $\mathbf{U}_s$, and the later (smaller) singular values $\mathbf{\Sigma}_n$ corresponding to the noise subspace $\mathbf{U}_n$. The singular values reflect the energy of the signal and the energy distribution of the noise, and help to determine the number of signals (the number of signals is usually determined by selecting the first K significant singular values). $\mathbf{V}$, $\mathbf{V}_s$, and $\mathbf{V}_n$ are their respective matrices of right singular vectors.

Then, the MUSIC spectral function P_{MUSIC} is constructed using the noise subspace or signal subspace obtained from the SVD decomposition:

$$P_{\mathrm{MUSIC}}(\theta) = \frac{1}{\mathbf{a}^{\mathrm{H}}(\theta)\mathbf{U}_n\mathbf{U}_n^{\mathrm{H}}\mathbf{a}(\theta)} \tag{28}$$

Finally, the locations of the peaks, which correspond to the angle of DOA of the incident signal, are found by calculating the $P_{\mathrm{MUSIC}}(\theta)$ at different angles. For analysis and comparison, (28) is normalized:

$$P'_{\mathrm{MUSIC}}(\theta) = 10\log_{10}\frac{|P_{\mathrm{MUSIC}}(\theta)|}{\max|P_{\mathrm{MUSIC}}(\theta)|} \tag{29}$$

From (28) and (29), it can be observed that the incidence direction of the signal source can be obtained by accurately finding either the signal subspace or the noise subspace provided the array steering vectors are known. In addition, by analyzing the distribution of the eigenvalues of the covariance, the number of signal sources can be effectively determined, thereby enabling accurate and stable estimation of the incidence directions of all signal sources.

Remark 5: In this paper, the MUSIC algorithm based on SVD is utilized. This spectral search algorithm effectively separates the signal and noise subspaces, enhances the resolution of the algorithm, and is particularly well-suited for scenarios involving complex multipath interference and low signal-to-noise ratios.

Remark 6: Similar to the conventional MUSIC algorithm, the proposed method remains sensitive to the number of signals due to its reliance on the noise subspace dimension during the spectral search stage. Therefore, it requires prior knowledge of the number of both coherent and uncorrelated signals. It is worth noting that several established techniques, such as the Akaike information criterion (AIC) and the minimum description length (MDL) criterion [33], [34], are available for accurate source number estimation. Integrating such methods with the proposed approach can facilitate fully blind DOA estimation of the target signals.

Remark 7: A key limitation of traditional information-theoretic methods (e.g., AIC and MDL) is their inability to handle coherent signals. Although spatial smoothing techniques can be used to pre-process the covariance matrix, and the smoothed matrix can then be used with AIC/MDL to estimate the total number of signals, the resulting estimate remains a combined count. Furthermore, these methods cannot accurately distinguish between coherent and uncorrelated signals. For this purpose, a spatial differencing matrix is built, after which a singular value-based ratio criterion can be utilized to independently estimate their respective numbers [35].

Based on the aforementioned content, the method proposed in this paper is summarized as follows, with its basic flow illustrated in Fig. 2. The steps are summarized below:

Rotation spatial differencing method

1) Estimate the array signal covariance matrix using the maximum likelihood method.

2) Construct a modified covariance matrix using the rotation matrix method.

3) Perform signal decoherence using the spatial differencing method.

4) Get the signal and noise subspaces by SVD.

5) Plot the signal spectrum using the signal spectral function.

6) Identify the spectral peaks in the signal spectrum to estimate the direction of signal incidence.

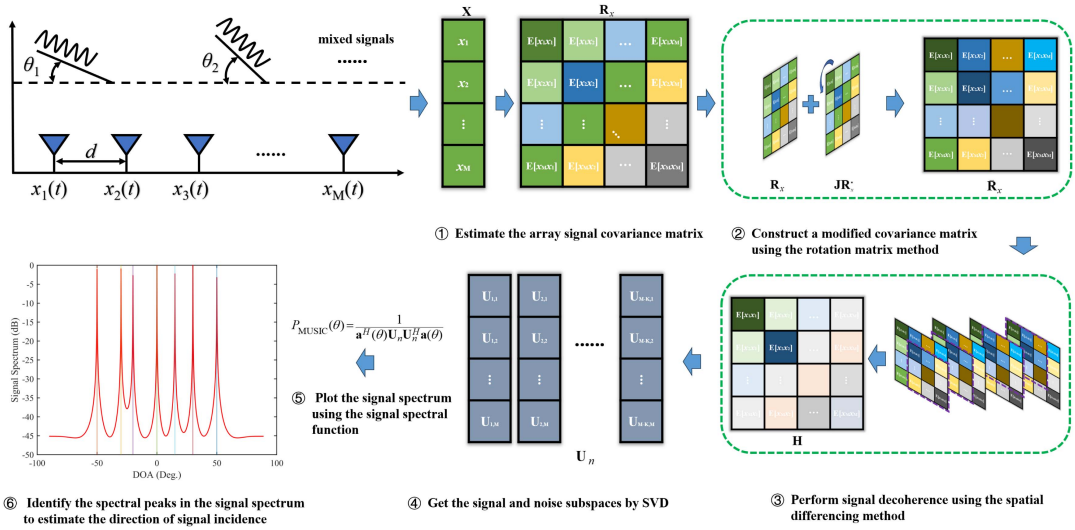

FIGURE 2. Rotation spatial differencing method.

IV. SIMULATION RESULTS

In order to verify the effectiveness of the proposed method, this section analyzes the estimation performance of the proposed method and identifies the key factors influencing its performance by setting up relevant experiments. In addition, the superiority of the proposed method in this paper is demonstrated through experimental comparisons.

A. EXPERIMENT I

In this section, the proposed method is compared with the Method 1 from Ref. [23] and the Method 2 from Ref. [32] as well as the conventional TMUSIC. A total of seven signals are set up in this simulation experiment, including four coherent signals with incident directions of $-30°$, $0°$, $10°$, and $40°$, and three uncorrelated signals with incident directions of $-45°$, $-10°$, and $60°$, respectively. In addition, the external noise is modeled as Gaussian white noise with 0 mean.

1) OVERALL ESTIMATED EFFECT

First of all, to demonstrate the effectiveness of the method proposed in this paper, a simulation experiment is set up, whose number of array sensors is selected as $M = 10$; the number of spatial differencing subarrays is $P = 2$; the signal to noise ratio (SNR) is selected as SNR $= 10$; the array sensor interval is half of the wavelength $d = \lambda/2$; and the number of snapshots is $N = 200$. The experimental results are presented as follows:

As shown in Fig. 3 that the method proposed in this paper accurately estimates the incident direction of the signal source, with higher spectral peaks and better resolution. In contrast, other methods demonstrate poor estimation accuracy or even fail.

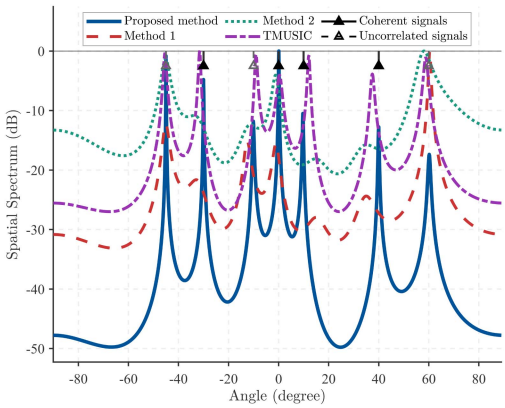

FIGURE 3. DOA spectral estimation of mixed signals ($M = 10$, $N = 200$, SNR $= 10$, $P = 2$).

2) DOA SPECTRAL ESTIMATION OF COHERENT SIGNALS

Fig. 4 shows the DOA estimation performance for different numbers of subarrays. It is evident that the method proposed in this paper has very accurate DOA estimation regardless of the number of subarrays. In contrast, Method 1 and Method 2 fail to accurately estimate the source direction when $P = 2$. The conventional TMUSIC can estimate the direction of the signal source, but the accuracy is relatively poor. Meanwhile, as the number of subarrays increases, all methods except TMUSIC show a significant improvement (the estimation of TMUSIC is independent of P, as it does not utilize spatial differencing techniques). Meanwhile, since Method 2 is based on Method 1 and employs the forward-backward spatial differencing approach, their estimation performances are similar. However, the proposed method in this paper consistently maintains high DOA resolution and estimation accuracy compared to the other three methods.

3) DOA SPECTRAL ESTIMATION OF UNCORRELATED SIGNALS

Fig. 5 illustrates the DOA estimation performance of the four methods for uncorrelated signals with different numbers of subarrays. It is evident that Methods 1 and 2 can not be able to

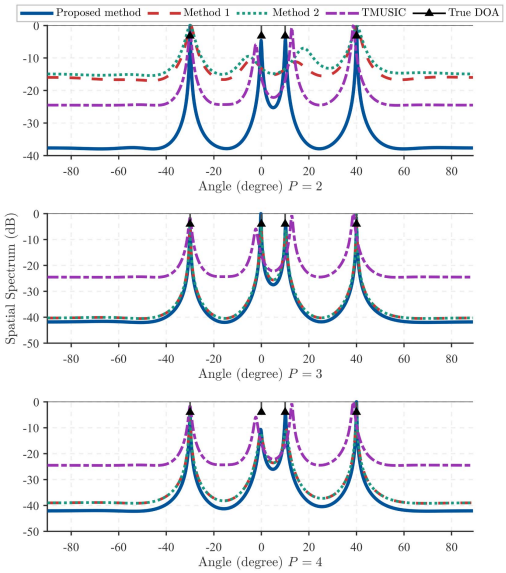

FIGURE 4. DOA spectral estimation of coherent signals for different number of subarrays ($M = 10, N = 200$, SNR $= 10$).

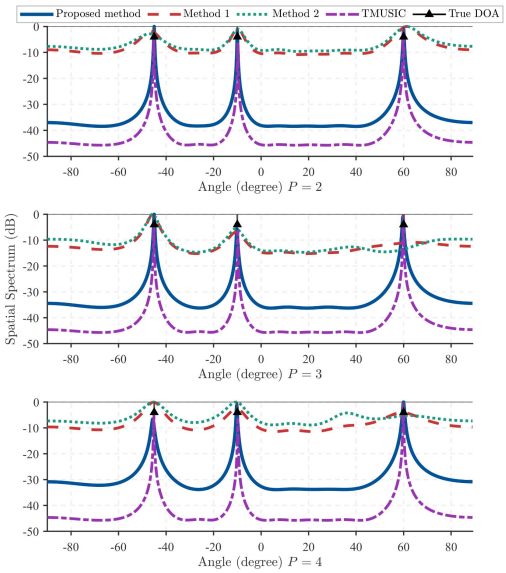

FIGURE 5. DOA spectral estimation of uncorrelated signals for different number of subarrays ($M = 10, N = 200$, SNR $= 10$).

discriminate the direction of incoming waves for uncorrelated signals. The conventional TMUSIC method provides the best estimation results. The proposed method in this paper also accurately estimates the direction of incoming waves, demonstrating its capability to handle uncorrelated signals. However, the improvement is not significant as the number of subarrays increases.

4) DETAILED PARAMETER ANALYSIS

Next, this section will examine the effect of various parameters on the estimation performance of the proposed method separately. At the same time, to more concretely demonstrate

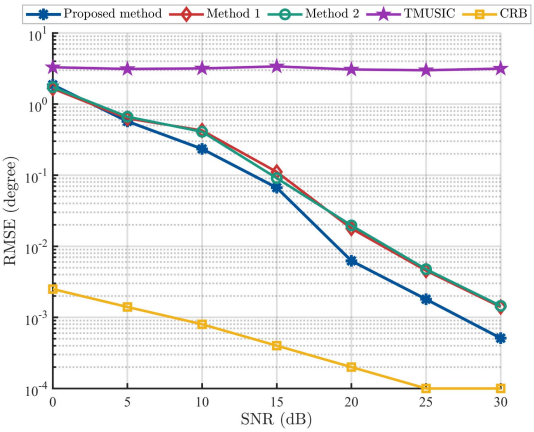

FIGURE 6. Variation of DOA-estimated RMSE with SNR ($M = 10, N = 200, P = 2$).

the superiority of the proposed method, the experimental results will be quantitatively analyzed using the root mean square error (RMSE). RMSE is defined as follows:

$$\text{RMSE} = \sqrt{\frac{1}{KT}\sum_{k=1}^{K}\sum_{t=1}^{T}\left(\theta_k - \hat{\theta}_k\right)^2} \tag{30}$$

where K is the number of sources; T is the number of Monte Carlo simulations (set to 500); $\hat{\theta}_k$ is the estimated value of DOA; and θ_k is the actual value of DOA. Additionally, the Cramér-Rao bound (CRB) from Ref. [36] is introduced as a benchmark for the DOA estimation.

Remark 8: As the main problem of DOA estimation for coherent signals targeted by these methods, the subsequent comparison experiments only analyze the DOA estimation performance of coherent signals. The DOA estimation of uncorrelated signals, on the other hand, follows similar patterns to the factors analyzed later, and therefore the description is not repeated.

Signal to noise ratio (SNR): As shown in Fig. 6, as the SNR increases, it is evident that the accuracy of the methods proposed in this paper also improves. There is also a significant increase in the estimation accuracy between Method 1 and Method 2. Meanwhile, due to the inherent limitations of the TMUSIC method, its estimation accuracy does not show significant improvement. In addition, compared to other methods, the proposed method consistently achieves higher estimation accuracy at the same SNR.

Number of snapshots (N): As shown in Fig. 7, it is evident that the estimation accuracy of these methods improves as the number of snapshots increases. Meanwhile, the proposed method consistently exhibits the best estimation accuracy at the same number of snapshots.

Number of array sensors (M): As shown in Fig. 8, it can be observed that the estimation accuracy of all methods improves with an increase in the number of array sensors, M. Meanwhile, the simulation experiments find that an increase in M results in higher resolution, greater spectral peak heights, and an expanded effective aperture. In addition, the proposed

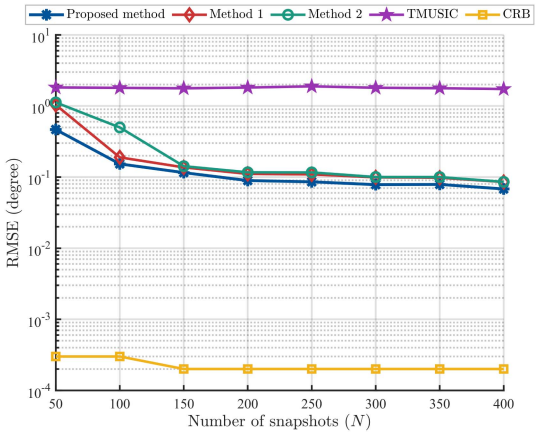

FIGURE 7. Variation of DOA-estimated RMSE with the number of snapshots ($M = 10$, SNR $= 20$, $P = 2$).

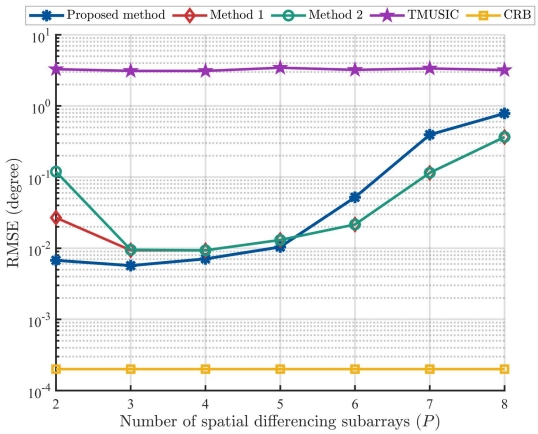

FIGURE 9. Variation of DOA-estimated RMSE with the number of spatial differencing subarrays ($M = 10$, $N = 200$, SNR $= 20$).

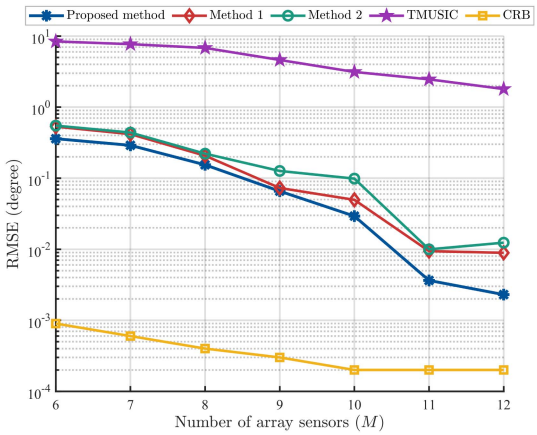

FIGURE 8. Variation of DOA-estimated RMSE with the number of array sensors ($N = 200$, SNR $= 20$, $P = 2$).

method demonstrates significantly better estimation performance compared to the other methods under the same number of array sensors.

Number of spatial differencing subarrays (P): As shown in Fig. 9, it is evident that the number of subarrays has a significant impact on the proposed method in this paper, Method 1 and Method 2; meanwhile, since TMUSIC does not use the spatial differencing technique, its estimation performance remains relatively unaffected. When the number of differential subarrays is chosen to be 3, the estimation accuracy of all methods in this paper except TMUSIC method is optimal. Beyond this point, the effect of the number of subarrays diminishes and may even lead to a decrease in estimation performance. However, the proposed method in this paper consistently achieves the highest estimation accuracy even with a lower number of subarrays.

Remark 9: Note that when the number of spatial differencing subarrays increases, their aperture decreases, which leads to a reduction in the number of sources that can be estimated. Meanwhile, when the number of subarrays is increased from 2 to 3, there is a significant improvement in estimation accuracy. However, further increases in the number of subarrays result in a decline in DOA estimation performance. Therefore, selecting an optimal number of subarrays is crucial to achieve accurate DOA estimation.

In summary, the DOA estimation method proposed in this paper demonstrates significant advantages over existing methods, including greater stability, higher accuracy, and more efficient estimation. Experimental analysis has shown that increasing the number of array sensors M results in higher and sharper spectral peaks, enhancing the array's resolution. Additionally, improvements in estimation accuracy are observed as the SNR and the number of snapshots N increase, along with the selection of an appropriate number of subarrays P.

Remark 10: Traditional spatial differencing methods require two separate one-dimensional spectral searches to estimate the DOAs of uncorrelated and coherent signals, respectively [23], [32]. The associated computational complexity is dominated by two SVDs—with complexities of $\mathcal{O}(M^3)$ and $\mathcal{O}((M-p+1)^3)$—as well as two one-dimensional spectral searches, with complexities of $\mathcal{O}(M^2)g_u$ and $\mathcal{O}((M-p+1)^2)g_c$. Here, g_u and g_c denote the number of grid points searched along the DOA axis for the uncorrelated and coherent signals, respectively. In contrast, the proposed method can simultaneously estimate both coherent and uncorrelated signals, requiring only one SVD of complexity $\mathcal{O}((M-p+1)^3)$ and a single one-dimensional spectral search of complexity $\mathcal{O}((M-p+1)^2)g_s$, where g_s represents the number of grid points used in the search for the mixed signals. As a result, the computational complexity is significantly reduced, enabling more efficient DOA estimation of the target signals.

B. EXPERIMENT II

In addition, in order to further demonstrate the advantages and characteristics of the proposed method in this paper, this section will modify (7) to conduct experimental comparisons using different data matrices ($\mathbf{R}_x + \mathbf{J}\mathbf{R}_x^*$, $\mathbf{R}_x$, $\mathbf{J}\mathbf{R}_x^*$). The

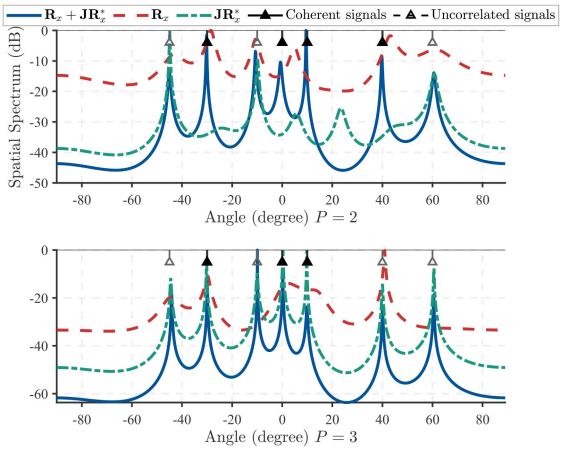

FIGURE 10. Estimation effects using three different covariance matrices ($M = 10, N = 200$, SNR $= 10$).

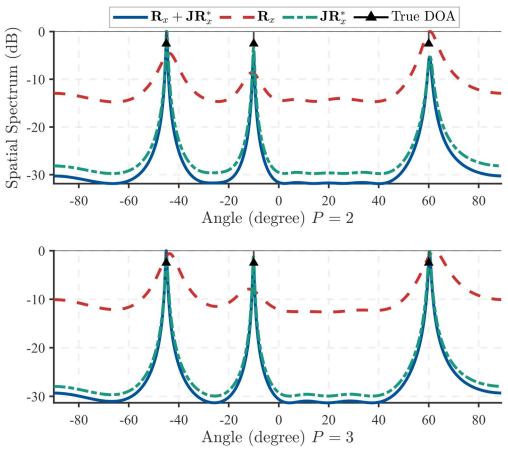

FIGURE 12. DOA spectral estimation of uncorrelated signals for different number of subarrays ($M = 10, N = 200$, SNR $= 10$).

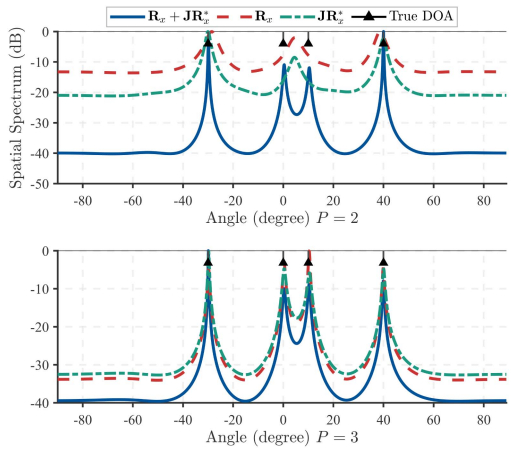

FIGURE 11. DOA spectral estimation of coherent signals for different number of subarrays ($M = 10, N = 200$, SNR $= 10$).

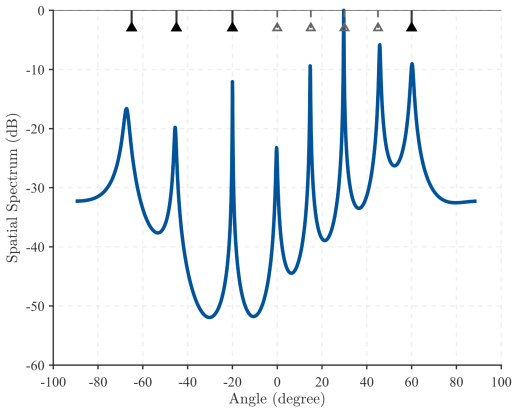

FIGURE 13. DOA spectral estimation of the maximum number of signal sources when $P = 2$ ($M = 10, N = 200$, SNR $= 10$); $K_{\max} = M - P = 8$; θ_{coherent} : $-65°, -45°, -20°, 60°$; $\theta_{\text{uncorrelated}}$: $0°, 15°, 30°, 45°$.

number of its array sensors and other parameters are consistent with Experiment I.

1) OVERALL ESTIMATED EFFECT

Fig. 10 show the estimated effects of DOA using the three covariance matrices with $P = 2$ and $P = 3$, respectively. It can be clearly seen that using $\mathbf{R}_x + \mathbf{JR}_x^*$ has an advantage when the number of subarrays is small. The analysis in Section III shows that $\mathbf{R}_x$ and $\mathbf{JR}_x^*$ have different structures. Combining the two to construct $\bar{\mathbf{R}}$ will make the newly composed modified covariance matrix increase the rank of the matrix without damaging the array flow pattern, thus initially realizing the decoherence of the signal. In addition, the number of subarrays also affects the upper limit of source estimation, reducing the number of sources that can be estimated when there are too many subarrays. Therefore, it is essential to be able to accurately estimate the direction of signal incidence with a small number of subarrays.

Figs. 11 and 12 show the results of incident direction estimation for coherent and uncorrelated signals with different number of subarrays, respectively. With these two figures it is equally demonstrated that the proposed method is able to estimate not only coherent signals but also uncorrelated signals when the number of subarrays is small. And its estimation accuracy and resolution are more excellent.

2) THE ABILITY OF IDENTIFIABILITY

Figs. 13 and 14 show the estimation of the maximum number of DOA-estimated sources for $P = 2$ and $P = 3$, respectively. According to Refs. [23], [31], [32], the maximum number of coherent signals that can be estimated should be less than the total number of sensors in each subarray, while the number of subarrays should be greater than or equal to the number of signals. Therefore, when $P = 2$, the maximum number of coherent signal sources that can be estimated is 2. Additionally, those methods are unable to estimate both coherent and uncorrelated signals simultaneously. Consequently, when sources are mixed (both coherent and uncorrelated signals), the maximum number that can be estimated at once by those methods is 2.

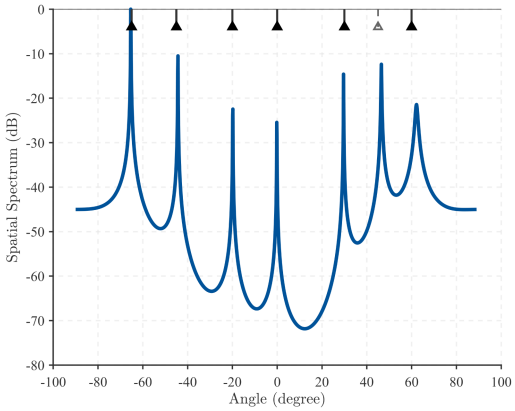

FIGURE 14. DOA spectral estimation of the maximum number of signal sources when $P = 3$ ($M = 10$, $N = 200$, SNR $= 10$); $K_{max} = M - P = 7$; $\theta_{coherent}$: $-65°, -45°, -20°, 0°, 30°, 60°$; $\theta_{uncorrelated}$: $45°$.

However, as shown in Figs. 13 and 14, the method proposed in this paper can estimate $M - P$ signal incidence directions at once. The maximum number of coherent signals that can be estimated is $2P$. This represents a significant improvement in estimation efficiency, capability, and accuracy.

V. CONCLUSION

In this paper, a DOA estimation method with high resolution is proposed for mixed signals of uncorrelated and coherent signals. It utilizes methods such as matrix rotation and spatial differencing to construct a new modified covariance matrix, and uses SVD-based MUSIC spectral search algorithm to achieve stable and accurate estimation. Compared with other existing methods, its estimation accuracy is higher and its resolution is better by having a more stable estimation process. In addition, this method is able to estimate the DOA directions of all mixed signals at one time, and has a fast and good stable estimation capability. However, its estimation performance is poor in the case of low signal-to-noise ratio, so in the next step, we will study the high-resolution algorithm in the case of low SNR and further investigate the DOA estimation under colored noise or broadband signals.

REFERENCES

[1] P. Kumari, J. Choi, N. González-Prelcic, and R. W. Heath, "IEEE 802 11ad-based radar: An approach to joint vehicular communication-radar system," *IEEE Trans. Veh. Technol.*, vol. 67, no. 4, pp. 3012–3027, Apr. 2018.

[2] J. H. Winters, "Smart antennas for wireless systems," *IEEE Pers. Commun.*, vol. 5, no. 1, pp. 23–27, Feb. 1998.

[3] Z. Zhang, M. Iskander, Z. Yun, and A. Host-Madsen, "Hybrid smart antenna system using directional elements–performance analysis in flat rayleigh fading," in *Proc. IEEE MTT-S Int. Microw. Symp. Dig.*, Oct., 2003, vol. 3, pp. 1537–1540.

[4] ChienHsiang Wu and Chin-Feng Lai, "A survey on improving the wireless communication with adaptive antenna selection by intelligent method," *Comput. Commun.*, vol. 181, pp. 374–403, Jan. 2022.

[5] Q. Xie, Z. Wang, F. Wen, J. He, and T.-K. Truong, "Coarray tensor train decomposition for bistatic MIMO radar with uniform planar array," *IEEE Trans. Antennas Propag.*, vol. 73, no. 8, pp. 5310–5323, Aug. 2025.

[6] Y. Fang, S. Zhu, Y. Gao, and C. Zeng, "DOA estimation for coherent signals with improved sparse representation in the presence of unknown spatially correlated Gaussian noise," *IEEE Trans. Veh. Technol.*, vol. 69, no. 9, pp. 10059–10069, Sep., 2020.

[7] X. Wu, W.-P. Zhu, and J. Yan, "A high-resolution DOA estimation method with a family of nonconvex penalties," *IEEE Trans. Veh. Technol.*, vol. 67, no. 6, pp. 4925–4938, Jun. 2018.

[8] R. Shafin, L. Liu, J. Zhang, and Y.-C. Wu, "DoA estimation and capacity analysis for 3-D millimeter wave massive-MIMO/FD-MIMO OFDM systems," *IEEE Trans. Wireless Commun.*, vol. 15, no. 10, pp. 6963–6978, Oct. 2016.

[9] T. DiPassio, M. C. Heilemann, and M. F. Bocko, "Direction of arrival estimation of an acoustic wave using a single structural vibration sensor," *J. Sound Vib.*, vol. 553, pp 117671, 2023.

[10] K. M. Wong, J. P. Reilly, Q. Wu, and S. Qiao, "Estimation of the directions of arrival of signals in unknown correlated noise. I the MAP approach and its implementation," *IEEE Trans. Signal Process.*, vol. 40, no. 8, pp. 2007–2017, Aug. 1992.

[11] K. Ma et al., "A wave-confining metasphere beamforming acoustic sensor for superior human-machine voice interaction," *Sci. Adv.*, vol. 8, 2022, Art. no. eadc9230.

[12] Q. Xie, J. Shi, F. Wen, and Z. Zheng, "Higher-order tensor decomposition for 2D-DOD and 2D-DOA estimation in bistatic MIMO radar," *Signal Process.*, vol. 238, Art. no. 110196, 2026.

[13] R. Schmidt, "Multiple emitter location and signal parameter estimation," *IEEE Trans. Antennas Propag.*, vol. AP-34, no. 3, pp. 276–280, Mar. 1986.

[14] G. Su and M. Morf, "The signal subspace approach for multiple wide-band emitter location," *IEEE Trans. Acoust., Speech, Signal Process.*, vol. ASSP-31, no. 6, pp. 1502–1522, Dec. 1983.

[15] P. Stoica, P. Babu, and J. Li, "SPICE: A sparse covariance-based estimation method for array processing," *IEEE Trans. Signal Process.*, vol. 59, no. 2, pp. 629–638, Feb. 2011.

[16] A. Das, "Real-valued sparse bayesian learning for off-grid direction-of-arrival (DOA) estimation in ocean acoustics," *IEEE J. Ocean. Eng.*, vol. 46, no. 1, pp. 172–182, Jan. 2021.

[17] M. Viberg, P. Stoica, and B. Ottersten, "Maximum likelihood array processing in spatially correlated noise fields using parameterized signals," *IEEE Trans. Signal Process.*, vol. 45, no. 4, pp. 996–1004, Apr. 1997.

[18] S. A. Vorobyov, A. B. Gershman, and K. M. Wong, "Maximum likelihood direction-of-arrival estimation in unknown noise fields using sparse sensor arrays," *IEEE Trans. Signal Process.*, vol. 53, no. 1, pp. 34–43, Jan. 2005.

[19] D. Kundu, "Modified MUSIC algorithm for estimating DOA of signals," *Signal Process.*, vol. 48, no. 1, pp. 85–90, 1996.

[20] A. Parian Mahnaz and G. Sedigheh, "ML1,2 -MUSIC algorithm for DOA estimation of coherent sources," *IET Signal Process.*, vol. 11, no. 4, pp. 429–436, 2017.

[21] F. Wen, J. Shi, G. Gui, C. Yuen, H. Sari, and F. Adachi, "Joint DOD and DOA estimation for NLOS target using IRS-aided bistatic MIMO radar," *IEEE Trans. Veh. Technol.*, vol. 73, no. 10, pp. 15798–15802, Oct. 2024.

[22] A. Liu, D. Yang, S. Shi, Z. Zhu, and Y. Li, "Augmented subspace music method for DOA estimation using acoustic vector sensor array," *IET Radar, Sonar Navigation*, vol. 13, no. 6, pp. 969–975, 2019.

[23] X. Ma, X. Dong, and Y. Xie, "An improved spatial differencing method for DOA estimation with the coexistence of uncorrelated and coherent signals," *IEEE Sensors J.*, vol. 16, no. 10, pp. 3719–3723, May 2016.

[24] W. Mao, G. Li, X. Xie, and Q. Yu, "DOA estimation of coherent signals based on direct data domain under unknown mutual coupling," *IEEE Antennas Wireless Propag. Lett.*, vol. 13, pp. 1525–1528, 2014.

[25] Tie-Jun Shan, M. Wax, and T. Kailath, "On spatial smoothing for direction-of-arrival estimation of coherent signals," *IEEE Trans. Acoust., Speech, Signal Process.*, vol. ASSP-33, no. 4, pp. 806–811, Aug. 1985.

[26] H. Wang and M. Kaveh, "Coherent signal-subspace processing for the detection and estimation of angles of arrival of multiple wide-band sources," *IEEE Trans. Acoust., Speech, Signal Process.*, vol. ASSP-33, no. 4, pp. 823–831, Aug. 1985.

[27] H. Chen, C.-P. Hou, Q. Wang, L. Huang, and W.-Q. Yan, "Cumulants-based toeplitz matrices reconstruction method for 2-D coherent DOA estimation," *IEEE Sensors J.*, vol. 14, no. 8, pp. 2824–2832, Aug. 2014.

[28] J. Zhang, M. Bao, J. Yang, Z. Chen, and H. Hou, "DOA tracking algorithm based on AVS pseudo-smoothing for coherent acoustic targets," *IEEE Trans. Aerosp. Electron. Syst.*, vol. 59, no. 6, pp. 8175–8193, Dec. 2023.
[29] I. Orr, M. Cohen, H. Damari, M. Halachmi, M. Raifel, and Z. Zalevsky, "Coherent, super-resolved radar beamforming using self-supervised learning," *Sci. Robot.*, vol. 6, 2021, Art. no. eabk0431.
[30] J. P. Merkofer, G. Revach, N. Shlezinger, T. Routtenberg, and R. J. G. van Sloun, "DA-MUSIC: Data-driven doa estimation via deep augmented MUSIC algorithm," *IEEE Trans. Veh. Technol.*, vol. 73, no. 2, pp. 2771–2785, Feb. 2024.
[31] F. Liu, J. Wang, C. Sun, and R. Du, "Spatial differencing method for DOA estimation under the coexistence of both uncorrelated and coherent signals," *IEEE Trans. Antennas Propag.*, vol. 60, no. 4, pp. 2052–2062, Apr. 2012.
[32] W. Rao, Feng-qin Jia, and D. Li, "DOA estimation of uncorrelated and coherent mixed signals in colored noise," *ACTA ELECTRONICA SINICA*, vol. 51, no. 3, pp. 622–631, 2023.
[33] D. Adionel Guimaraes, P. Maria Soares, and R. A. A. Souza, "An empirical method for estimating the number of signal sources," *IEEE Latin Amer. Trans.*, vol. 13, no. 7, pp. 2057–2064, Jul. 2015.
[34] A. Guimarães Dayan and A. A. Rausley de, "Simple and efficient algorithm for improving the MDL estimator of the number of sources," *Sensors*, vol. 14, no. 10, pp. 19477–19492, 2014.
[35] H. Tao, J. Xin, Jiasong Wang, N. Zheng, and A. Sano, "Estimation of the number of narrowband signals in the presence of multipath propagation," in *Proc. IEEE 7th Sensor Array Multichannel Signal Process. Workshop*, 2012, pp. 489–492.
[36] Z. Ye, Y. Zhang, and C. Liu, "Direction-of-arrival estimation for uncorrelated and coherent signals with fewer sensors," *IET Microw., Antennas Propag.*, vol. 3, no. 3, pp. 473–482, 2009.

PENG LUO received the B.E. degree in mechatronic engineering from the Chongqing University of Technology, Chongqing, China, in 2021, and the M.E. degree in naval architecture and ocean engineering from Jimei University, Xiamen, China, in 2024. He is currently working toward the Ph.D. degree with the School of Naval Architecture, Ocean, and Civil Engineering, Shanghai Jiao Tong University, Shanghai, China. His research interests include array signal processing, direction-of-arrival (DOA) estimation, and underwater acoustic signal processing.

BOYU PANG received the B.S. degree from the Dalian University of Technology, Dalian, China, in 2019, and the Ph.D. degree in physical electronics from the Shanghai Institute of Technical Physics, Chinese Academy of Sciences, Shanghai, China, in 2024. She is currently a Postdoctoral Research Fellow with Shanghai Jiao Tong University, Shanghai, China. Her research interests include remote sensing image processing, super-resolution imaging, and signal processing.

DEFENG WU (Senior Member, IEEE) received the B.E. degree in automatic control and the Ph.D. degree in control theory and control engineering from Dalian Maritime University, Dalian, China, in 2005 and 2010, respectively. From 2008 to 2009, he was a Visiting Ph.D. Student with the School of System Engineering, University of Reading, Reading, U.K. From 2011 to 2015, he was a Lecturer with the School of Marine Engineering, Jimei University, Xiamen, China. He also acted as a Visiting Scholar with the Illinois Institute of Technology, Chicago, IL, USA, from 2015 to 2016. From 2015 to 2019, he was an Associate Professor with Jimei University, where he is currently a Full Professor. He has authored or coauthored more than 70 research papers in reputed Science Citation Index journals. His current research interests include systems and control theory, signal processing, machine learning, reinforcement learning, and computational intelligence, with applications in marine engineering.

W. ZENG is currently a Full Professor with Shanghai Jiao Tong University, Shanghai, China. His research focuses on signal processing.